AIP | Applied Physics Letters

Increased mobility for layer-by-layer transferred chemical vapor deposited graphene/boron-nitride thin films

Osama M. Nayfeh, A. Glen Birdwell, Cheng Tan, Madan Dubey, Hemtej Gullapalli, Zheng Liu, Arava Leela Mohana Reddy, and Pulickel M. Ajayan

Citation: Applied Physics Letters **102**, 103115 (2013); doi: 10.1063/1.4794533
View online: http://dx.doi.org/10.1063/1.4794533
View Table of Contents: http://scitation.aip.org/content/aip/journal/apl/102/10?ver=pdfcov
Published by the AIP Publishing

Increased mobility for layer-by-layer transferred chemical vapor deposited graphene/boron-nitride thin films

Osama M. Nayfeh,[1] A. Glen Birdwell,[1] Cheng Tan,[1] Madan Dubey,[1,a)] Hemtej Gullapalli,[2] Zheng Liu,[2] Arava Leela Mohana Reddy,[2] and Pulickel M. Ajayan[2,a)]
[1]*U.S. Army Research Laboratory (ARL), Sensors and Electron Devices Directorate (SEDD), 2800 Powder Mill Road, Adelphi, Maryland 20783, USA*
[2]*Department of Mechanical Engineering and Materials Science, Rice University, 6100 Main Street, Houston, Texas 77005, USA*

(Received 26 July 2012; accepted 22 February 2013; published online 15 March 2013)

Large-area chemical vapor deposited graphene/boron-nitride (G/BN) thin films are co-transferred layer-by-layer to silicon-di-Oxide (SiO_2) substrates, and transistors are constructed and examined. Raman spectra and high resolution transmission electron microscopy imaging show films of high quality. The graphene/boron-nitride/SiO_2 devices have a significantly increased peak electron/hole mobility of 3400/2200 cm^2/Vs with a reduced effective doping density over reference graphene/SiO_2 devices. The mobility dependence as a function of carrier density is compared with a physically based empirical model and is in agreement with the improvements due to a consistent reduction in the substrate induced phonon and impurity scattering and an improvement in the overall surface quality owed to the boron-nitride interlayer that separates the graphene from the SiO_2. Large-area G/BN thin films are promising for future high performance thin film electronic devices. [http://dx.doi.org/10.1063/1.4794533]

Large area, atomically-thin, graphene (G) synthesized by chemical vapor deposition and transferred to arbitrary rigid or flexible substrates is potentially useful for future ubiquitous electronic devices.[1–3] For CVD G on SiO_2 the mobility is typically reported to be less than 1000 cm^2/Vs. In addition to its polycrystalline structure, the degradation is attributed to extrinsic factors such as the substrate interaction and chemical modification due to impurities introduced during synthesis, transfer, and/or processing.[4–6] The latter can be mitigated by controlling growth/anneal conditions and the transfer process/cleaning.[6] The former, however, requires the use of separating inter-layers between the graphene and underlying substrate or complete suspension. Owing to an expected low level of surface dangling bonds, high energy optical phonon modes, and a lattice structure similar to graphene,[7] two dimensional (2D) hexagonal h-BN is emerging as a promising interlayer for the realization of high mobility substrate supported graphene. Recently Dean *et al.*[8] have observed mobility >5000 cm^2/Vs using precisely aligned graphene/boron-nitride (G/BN) micro-flakes, and Mayorov *et al.*[9] have provided evidence for micro-scale ballistic transport for G encapsulated in BN. Gannett *et al.*[10] and Kim *et al.*[11] have also recently demonstrated enhanced mobility using CVD graphene transferred onto exfoliated BN micro-flakes. However, the use of exfoliated BN micro-flakes poses challenges for large-area manufacturing of G/BN. In this study, thin films produced by layer-by-layer transferring of both Cu catalyzed large-area CVD graphene and large-area CVD BN are synthesized and examined. There is a significantly increased mobility over reference G/SiO_2 devices. The improvements are consistent with a reduction in substrate induced phonon and impurity scattering and an improvement in the overall surface quality owed to the use of the BN interlayer. While the mobility appears to still be limited by intrinsic quality and residual impurities, large area graphene/BN films could be promising for future high performance device and circuit applications.

Graphene and BN films are grown via low pressure chemical vapor deposition (LPCVD) on separate copper (Cu) foil using the methods in Refs. 12 and 13. After annealing at 950 °C in 500 mTorr Ar/H_2, 150 mTorr hexane (C_6H_{14}) vapor is released into the quartz tube for ~10 min followed by cooling to room temperature in argon/hydrogen (Ar/H_2). Similarly, for the growth of BN, the foils are annealed at 1000 °C for 20 min, and ammonia borane (NH_3-BH_3) precursor is sublimated at 130 °C and then carried into the reaction region by Ar/H_2 flow for 10-30 min. After BN growth, the furnace is quickly cooled down to room temperature, and separate samples are transferred to appropriate substrates for characterization. BN and graphene samples grown on Cu substrate are transferred layer-by-layer onto SiO_2/n+ Si substrates. The BN and graphene containing Cu foils are coated with poly methyl methacrylate (PMMA) separated, and then etched in dilute HNO_3 to dissolve the Cu. PMMA/BN films are first transferred to SiO_2/n+ Si substrates, and then the PMMA is dissolved using acetone and sequential isopropyl alcohol (IPA) rinses. Later, PMMA/graphene films are similarly transferred onto the prepared BN/SiO_2 substrates to produce a graphene/BN thin film.

Graphene/BN films are characterized by Raman spectroscopy using a WITec Alpha 300RA system under high intensity, low noise settings and are shown in Fig. 1(a). Spectra are measured in the backscattering configuration using the 532 nm line of a frequency-doubled Nd:YAG laser as the excitation source (~1.5 mW at sample) with a 100× objective and 600 grooves/mm grating with 0.5 s integration time. For direct comparison, spectra are taken on graphene-only and BN-only films. G/BN films have characteristic G related peaks and a BN related peak at ~1365 cm^{-1} consistent with the BN-

a)Authors to whom correspondence should be addressed. Electronic addresses: madan.dubey@us.army.mil and ajayan@rice.edu.

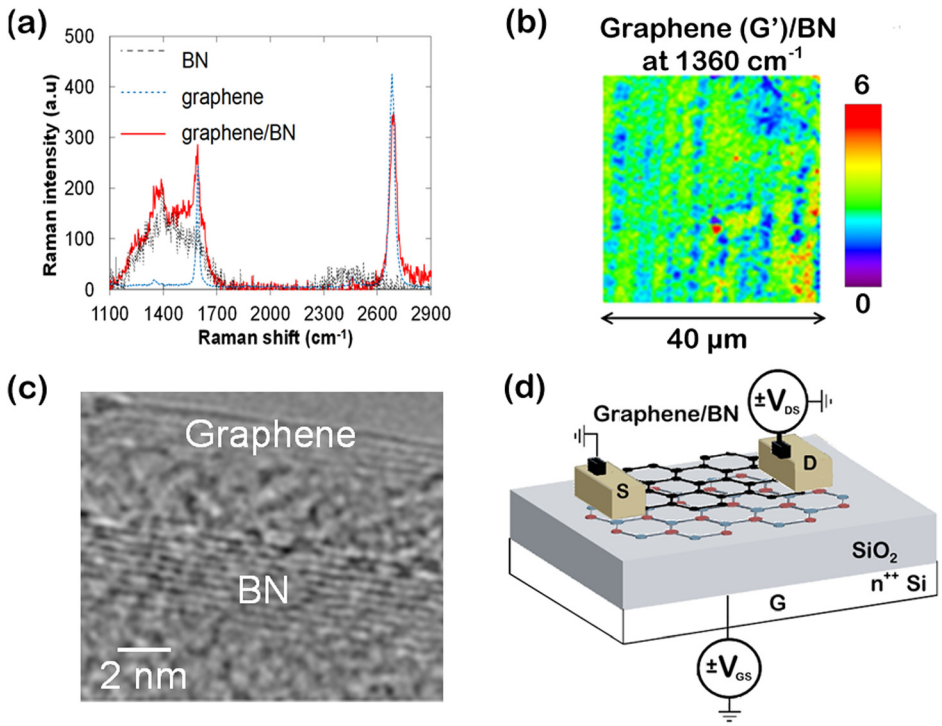

FIG. 1. (a) Representative Raman spectra of graphene/BN, BN-only, and graphene-only samples. (b) Raman map over a 40 μm (120 pixel) region of the intensity ratio of the graphene (G′)/BN@1365 cm^{-1} peaks. (c) HRTEM image of a segment of a graphene/BN thin film with a 4-5 nm gap is showing 4-layers G/8-layers BN. (d) Transistor schematic and biasing with L = 30 μm and W = 100 μm.

only spectra and with the reports in Refs. 13 and 14. The graphene G′/G peak intensity ratio ~1 with a G′ full-width-half-maxima (FWHM) ~45-60 cm^{-1} indicates Bi or multi layers graphene and the D/G ratio <0.1 points to a low defect density. There is minimal deviation of the G′ and G peak positions for the graphene-only films as compared to G/BN, evidence of low-levels of additional doping of the graphene due to the underlying BN. However, the change observed in peak ratio between the G and G′ peaks is difficult to quantify. Significant changes in this parameter can be observed in spectra collected at different regions within the same sample. These variations are a possible consequence of the transfer process. Fig. 1(b) shows a Raman map of the graphene (G′)/BN (~1365 cm^{-1}) peak intensities demonstrating good large-area graphene/BN uniformity. HRTEM characterization is also performed on graphene/BN films. The samples for HRTEM are prepared by first transferring graphene and BN on to SiO_2 substrate, which is then etched out using buffered hydrofluoric acid (buffered HF) followed by lifting off the G/BN films on to a transmission electron microscope (TEM) grid. Fig. 1(c) shows an HRTEM image in a segment where a 4-5 nm gap is present allowing for the graphene/BN films to be clearly distinguished from each other and is the clear indication of layer-by-layer transfer process. The gap is not intrinsic to the system and is observed only at certain regions which may be due to traces of residual PMMA on graphene. The graphene and BN films vary between double and multi-layers across samples.

Long gate length (L) and wide (W) transistor test structures (L = 30 μm and W = 100 μm) are constructed using the process flow reported in Ref. 6 using titanium/gold (Ti/Au) source/drain contacts and the n+ Si as the back-gate. A schematic of the devices is shown in Fig. 1(d). The devices were first dehumidified by placing in a desert cryogenics system for 15 h under vacuum and 400 K.[6] *In situ* electrical measurements are then performed using a Keithley 4200. Fig. 2(a) shows representative transfer (I_d vs. V_{gs}) characteristics of graphene/BN devices with a minimum conductivity Dirac point voltage $V_{dp} = 30$ V and near symmetric ambipolar electron/hole branches of the current characteristics. For comparison, the typical position of the Dirac point for graphene/SiO_2 devices is >75 V due to increased effective p-type doping.[15] Fig. 2(b) shows the measured output (I_d vs. V_{ds}) characteristics with Ohmic behavior at low V_{ds} and signs of the onset of saturation-like behavior with $V_{ds} > 3$ V. Such signs of saturation are typically not observed for reference graphene/SiO_2 devices. The field-effect mobility μ_{fet} is extracted from the measured transconductance, g_m under low lateral field conditions, $V_{ds} = 100$ mV using $\mu_{fet} = \frac{g_m L}{V_{ch} \cdot C_{ox} \cdot W}$, where W and L are the effective channel width and length of the device, respectively. The electron/hole charge density in the ambipolar channel is extracted using $N_{amb} = |C_{ox}(V_{gs} - V_{dp})|$, where C_{ox} is the total oxide capacitance. V_{ch} is the total potential drop across the channel, extracted from the applied V_{ds} and corrected for the drop across the contacts, V_{ct}. The typical contact resistance measured from transfer length measurement (TLM) measurements is 120 ± 25 Ω μm. The peak electron/hole mobility for graphene/BN is 3400 and 2200 cm^2/Vs and is

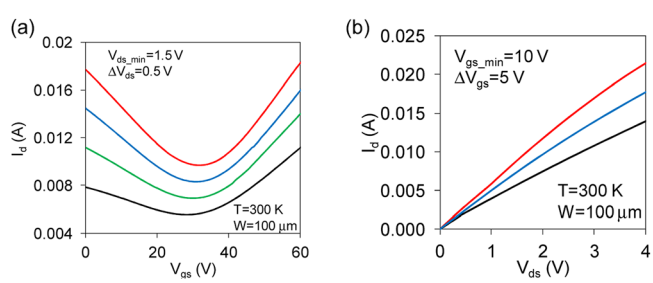

FIG. 2. Measured electrical characteristics for a representative graphene/BN transistor test structure shown schematically in Fig. 1(d): (a) transfer (I_d vs. V_{gs}) characteristics with near symmetric electron/hole branches of the current and a Dirac point located near 30 V and (b) output (I_d vs. V_{ds}) characteristics showing the onset of saturation-like behavior with $V_{ds} > 3$ V.

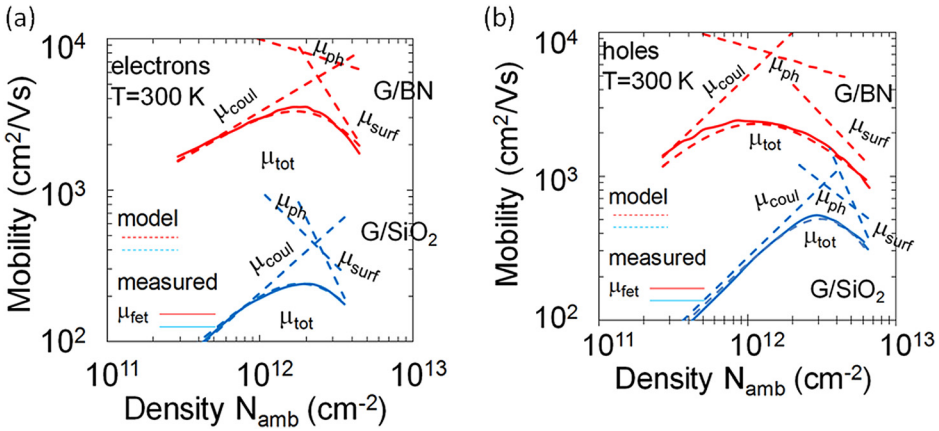

FIG. 3. Measured vs. modeled (a) electron and (b) hole mobility for graphene/BN and graphene/SiO_2 samples as a function of the extracted carrier density and the isolated Coulomb, phonon and surface mobility components. There is significantly enhanced carrier mobility for graphene/BN due to a consistent reduction in the substrate induced scattering and an improvement in the surface quality.

significantly increased over reference graphene/SiO_2 devices with a mobility less than 1000 cm^2/Vs.[6]

The mobility density dependence is examined using physically based empirical expressions consistent with Coulomb, phonon, and surface roughness scattering components using Matthiessen's Rule, $\mu_{tot}^{-1} = \mu_{coul}^{-1} + \mu_{surf}^{-1} + \mu_{ph}^{-1}$. This model has been shown to produce good agreement with the experimental mobility on several substrates.[3] Figs. 3(a) and 3(b) show the measured and modeled electron/hole mobility of graphene/BN and reference graphene/SiO_2 devices. The mobility increases with increasing density, and μ_{coul} obeys a Coulomb scattering type power law $\mu_{coul} = AN_{amb}^{\alpha}$, where α is the degree of screening. There is an increase in μ_{coul} for graphene/BN consistent with a reduced substrate induced impurity scattering. Additionally, there is a reduction also in α for graphene/BN (0.6 vs. 0.9) pointing to the presence of Coulomb contributions that are both substrate-induced and from impurities.[15] While substrate doping is reduced for G/BN over G/SiO_2 bringing V_{dp} significantly closer to neutral, there is persistent residual p-type doping and Coulomb scattering due to residual moisture and resist residue trapped between the graphene and BN as well as any oxygen species incorporated during processing/growth.[6] The phonon mobility is $\mu_{ph} = P \cdot N_{amb}^{\beta}\left(\frac{T}{300}\right)^{\gamma}$ where P is a fit parameter, T is the temperature, and γ and β are in principle determined by the electronic structure and phonon coupling with the substrate. There is also an increase in the phonon mobility for graphene/BN and manifested as a modulation in β (-0.3 vs. -1). This is consistent with the expected larger optical phonon energy modes for BN over SiO_2.[8] While the overall μ_{ph} is improved, it remains reduced from the giant values reported for exfoliated micro-flakes, and this deviation can be attributed to the intrinsic polycrystalline structure of the CVD material and relatively elevated defect levels. In addition to an overall increase in μ_{ph} the mobility degrades at high density and obeys a surface roughness scattering inverse power law $\mu_{surf} = \frac{\delta}{N_{amb}{}^{\Delta}}$, where δ is a fit parameter and Δ is the degree of roughness. Good agreement is obtained using $\Delta = 1.2$ for G/BN whereas $\Delta = 2.1$ on graphene/SiO_2 consistent with an overall improved surface quality for G/BN.

Large-area G/BN thin films are prepared by CVD growth on Cu foils and layer-by-layer transferring. Material metrology reveals films of high quality and representative of a ly transferred G/BN thin film. G/BN devices have significantly increased carrier mobility and a reduced effective doping density over reference G/SiO_2 devices. Examination of the density dependency of the mobility shows that the gains are consistent with an improved G/BN substrate interaction that reduces the level of impurity and phonon scattering in addition to an overall improvement in the surface quality.

The authors acknowledge the support of the Army Research Lab (ARL) Director's Strategic Initiative (DSI) program on graphene nanoelectronics. Device processing/characterization and Raman measurement was performed using the ARL device fabrication and nano-electronics laboratories. P.M.A. and Z.L. also acknowledge funding support from the ONR MURI program on graphene. The views and conclusions contained in this document are those of the authors and should not be interpreted as representing the official policies, either expressed or implied, of the ARLor the U.S. Government. The U.S. Government is authorized to reproduce or distribute reprints for Government purposes notwithstanding any copyright notation herein.

[1]X. S. Li, W. W. Cai, J. H. An, S. Kim, J. Nah, D. X. Yang, R. Piner, A. Velamakanni, I. Jung, E. Tutuc, S. K. Banerjee, L. Colombo, and R. S. Ruoff, Science **324**, 1312 (2009).
[2]S. Bae, H. K. Kim, Y. B. Lee, X. F. Xu, J. S. Park, Y. Zheng, J. Balakrishnan, T. Lei, H. R. Kim, Y. Song, Y.-J. Kim, K. S. Kim, B. Ozyilmaz, A.-H. Ahn, B. H. Hong, and S. Ijima, Nat. Nanotechnol. **5**, 574–578 (2010).
[3]O. M. Nayfeh, IEEE Electron Device Lett. **32**(10), 1349–1351 (2011).
[4]M. I. Katsnelson and A. K. Geim, Philos. Trans. R Soc. A **366**, 195–204 (2008).
[5]S. Adam, E. H. Hwang, and S. D. Sarma, Physica E **40**, 1022–1025 (2008).
[6]O. M. Nayfeh, IEEE Trans. Electron Devices **58**(9), 2847–2853 (2011).
[7]J. Xue, J. Sanchez-Yamagishi, D. Bulmash, P. Jacquod, A. Deshpande, K. Watanabe, T. Tanigushi, P. Jarillo-Herrero, and B. J. LeRoy, Nat. Mater. **10**, 282–285 (2011).
[8]C. R. Dean, A. F. Young, I. Meric, C. Lee, L. Wang, S. Sorgenfrei, K. Watanabe, T. Taniguchi, P. Kim, K. L. Shepard, and J. Hone, Nat. Nanotechnol. **5**, 722–726 (2010).
[9]A. S. Mayorov, R. V. Gorbachev, S. V. Morozov, L. Britnell, R. Jalil, L. A. Ponomarenko, P. Blake, K. S. Novoselov, K. Watanabe, T. Tanigushi, and A. K. Geim, Nano Lett. **11**, 2396–2399 (2011).
[10]W. Gannett, W. Regan, K. Watanabe, T. Tanigusihi, M. F. Crommie, and A. Zettl, Appl. Phys. Lett. **98**, 242105 (2011).
[11]E. Kim, T. Yu, E. Song, and B. Yu, Appl. Phys. Lett. **98**, 262103 (2011).
[12]H. Gullapalli, A. L. M. Reddy, S. Kilpatrick, M. Dubey, and P. M. Ajayan, Small **7**, 1697 (2011).
[13]L. Song, L. Ci, H. Lu, P. B. Sorokin, C. Jin, J. Ni, A. G. Kvashnin, D. G. Kvashnin, J. Lou, B. I. Yakobson, and P. M. Ajayan, Nano Lett. **10**(8), 3209–3215 (2010).
[14]L. Ci, L. Song, C. H. Jin, D. Jariwala, D. X. Wu, Y. J. Li, A. Srivastava, Z. F. Wang, K. Storr, L. Balicas, F. Liu, and P. M. Ajayan, Nat. Mater. **9**, 430–435 (2010).
[15]O. M. Nayfeh, T. Marr, and M. Dubey, IEEE Electron Device Lett. **32**(4), 473–475 (2011).